Fast Concomitant Gradient Field Correction for Spiral Scans

J. Y. Cheng[1], J. M. Santos[1], and J. M. Pauly[1]
[1]Department of Electrical Engineering, Stanford University, Stanford, CA, United States

Introduction: A major drawback to non-Cartesian imaging is the off-resonance blurring effects. Common linear techniques that remove the distortion effects are not sufficient, because the high order concomitant gradient fields are nontrivial for low fields and for scans that are more than 5 cm off isocenter [1]. Previous correction algorithms either are slow or do not take into account the known effects of concomitant gradient fields [3-5]. In this work, two fast and accurate algorithms to account for the concomitant field effects are presented and analyzed: one in the frequency domain [4] and the other in the spatial domain [3].

Methods: The concomitant gradient field distortion can be approximated as a quadratic phase function: $f(x,y,z,t) = K * g_m^2(t) * C(x,y,z)$, where K is a constant scaling factor, $g_m(t)$ is the total gradient magnitude for the spiral trajectory, and $C(x,y,z)$ is the spatial location effects of the concomitant gradient fields [2]. In order to reduce the computation time, the correction algorithm is performed post gridding since the value g_m^2 is smoothly varying as a function of *k*-space location.

The blurring correction was performed in both the *k*-space domain and the image domain for comparison. In the *k*-space domain approach, a series of images were generated by focusing each image with different center frequencies. The series was then spliced together for a final corrected image. In the spatial domain approach, the image was convolved with a spatial varying correction convolution kernel. For speed, these kernels can be precomputed and stored in a look-up table.

The experiment was performed using a GE resolution phantom in an 1.5T GE Signa EXCITE scanner. A spiral trajectory with 16 interleaves, a FOV of 20 cm, a TE/TR of 3.84/22.32 ms, and a resolution size of 0.8 mm was used to obtain a 5.88 mm slice using a multi-coil. Using *C++*, the data from each coil was gridded and corrected separately before the final image was reconstructed using the sum of squares.

Results and Discussion: The *k*-space domain and the image domain approach yielded the same improvement. The image domain approach, however, allowed for more frequency bins with no extra computation cost. Therefore, with a small increase of memory use for storing more kernels, accuracy can be improved without sacrificing speed. For the *k*-space domain approach, 10 frequency bins were used for an average correction time of ~0.4 s. For the image domain approach, 250 kernels with a width size of 20 were used for an average of ~0.1 s. The computation time can be further reduced by decreasing the number of bins in the *k*-space domain approach or by decreasing the kernel width in the image domain approach. Care must be taken not to induce artifacts.

In accordance with theory, the portions of the image furthest from isocenter in the *z*-direction demonstrated the most blurring and the most spatial warping. As seen in the figures, the distortion was corrected in the image while leaving the portions of the image near isocenter undistorted. In *Figures (D), (G),* and *(F)*, the high resolution data of the comb was mostly recovered using this correction method.

The residual blurring in the images can be partially attributed to B_0 inhomogeneities which can be accounted for using a linear field map on the phase corrected images [1]. The amount of *z* offset was emphasized in the figures through the spatial warping due to the gradient nonlinearities. Fortunately, the warping did not have a noticeable effect on the correction algorithm, because the off-resonance blurring varied slowly spatially and the warping error introduced only negligible terms in the high order concomitant gradient fields. The final image can be later unwarped using any unwarping algorithm.

Conclusion: The concomitant field distortion correction is preferably performed in the image domain due to its speed and accuracy. The algorithm corrects for most of the off-isocenter distortions. More work still needs to be done to include residual effects from B_0 inhomogeneities and gradient non-linearities.

References: [1] Chen *et al*, MRM 60, 2008. [2] King *et al*, MRM 41, 1999. [3] Ahunbay and Pipe, MRM 44, 2000. [4] Man *et al*, MRM 37, 1997. [5] Bernstein *et al*, MRM 39, 1998. [6] Du *et al*, MRM 48, 2002.

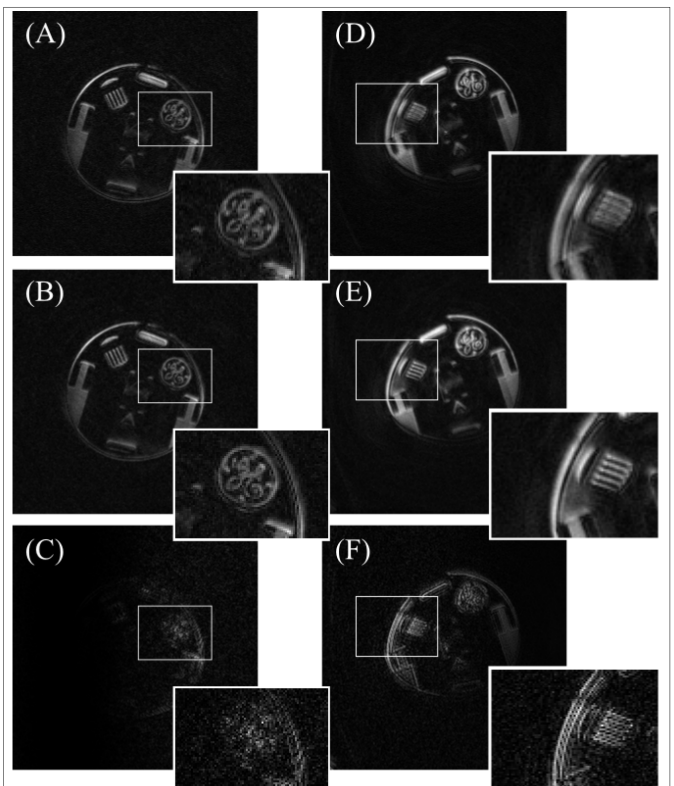

The resolution phantom was scanned in the sagittal orientation. **(A)**, **(B)**, and **(C)** are with a *z* offset of -58 mm acquired with a 4-channel coil. **(D)**, **(E)**, and **(F)** are with a *z* offset of -109 mm acquired with an 8-channel coil. **(A)** and **(D)** are the uncorrected images. **(B)** and **(E)** are the corrected images using an image domain approach. **(C)** and **(F)** are the difference images.